International Journal of Electrical and Power Engineering 2 (1): 39-49, 2008
ISSN: 1990-7958

Matrix Converter Based Variable Speed Wind Generator System

[1]K. Ghedamsi, [1]D. Aouzellag, [2]E.M. Berkouk
[1]Department of Electrical Engineering, A. Mira University, 06000 Bejaïa, Algeria
[2]Laboratory of Control Process, E.N.P, Algiers, Algeria

Abstract: In this study, a grid connected Variable Speed Wind Generation (VSWG) scheme using a Doubly Fed Induction Generator (DFIG) associated to a Flywheel Energy Storage System (FESS) is investigated. Therefore, the dynamic behaviour of a wind generator, including models of the wind turbine (aerodynamic), DFIG, AC/AC direct converter, converter control (algorithm of Venturini) and power control is studied. This study investigates also, the control method of the FESS with a classical squirrel-cage induction machine associated to a VSWG. Simulation results of the dynamic models of the wind generator are presented, for different operating points, to show the good performance of the proposed system.

Key words: Matrix converter, doubly fed induction generator, variable speed wind turbine, power control, flywheel energy storage system

INTRODUCTION

The last decades have seen a significant expansion of the use of the Wind Energy Conversion System (WECS). This is due, to the fact that this energy yields the production of electricity without any gas emission (Seyoum and Grantham, 2003; Aouzellag *et al*., 2006; Tounzi, 1998).

There are several reasons for using variable-speed operation of wind turbines. Among them, we notice possibilities to decrease stresses of the mechanical structure and acoustic noise reduction and the possibility to control active and reactive power (Seyoum and Grantham, 2003). Most of the major wind turbine manufactures are developing new larger wind turbines in the 3-6-MW range. These large wind turbines are all based on variable-speed operation with pitch control using a direct-driven synchronous generator (without gear box) or a doubly-fed induction generator. The major advantage of the DFIG is that the power electronic equipment only has to drive a part (20-30 %) of the total system power (Muljadi *et al*., 1998); this means that the losses in the power electronic converters are reduced as well as the cost.

This study introduces a direct AC-AC matrix converter, as an alternative to the conventional AC-DC-AC converter, for the wind turbine driving a DFIG (Aimani, 2003). The Matrix Converter (MC) eliminates the DC-link components and inherently resolves the size, weight and reliability issues and also provides an option for design of the converter as a compact/modular unit. The main advantages of MC are adjustable power factor (including unity), bidirectional power flow and the possibility of a more compact product (Schuster, 1998). The classical algorithm of venturini control of the MC is used (Alesina and Venturini, 1988).

The energy can be stored as kinetic energy in a rotating mass, which is called a flywheel. The flywheel is coupled to an electrical generator, which produces electricity when breaking the flywheel. FESS have thus found a specific application for the electrical power quality, as far as the voltage and frequency of their high dynamics, long lifetime and good efficiency; Flywheel Energy Storage Systems (FESSs) are well suited for short-term storages systems, which are generally sufficient to improve the electrical power quality. (Venturini, 1980; Alesina and Venturini, 1988; Hebner, 2002) The FESSs are suitable for improving the quality of the electrical power delivered by the wind generators and for helping these generators to contribute to the ancillary services (Cimuca, 2004).

In this study, we develop a model to study and to simulate the behaviour of the VSWG associated to FSSE connected to the grid. Firstly, we show the wind generator (wind turbine, gearbox, DFIG, MC and filters) (Aouzellag *et al*., 2006; Ghedamsi *et al*., 2006). Secondly, we present the Maximum Power Point Tracking (MPPT) algorithm to maximize the generated power. Thirdly, we expose the power control algorithm, as well as the RST regulator. In order to control active and reactive power exchange between the wind generator and the grid, a vector-control strategy will be presented. Fourthly, we present

Corresponding Author: K. Ghedamsi, Department of Electrical Engineering, A. Mira University, 06000 Bejaïa, Algeria

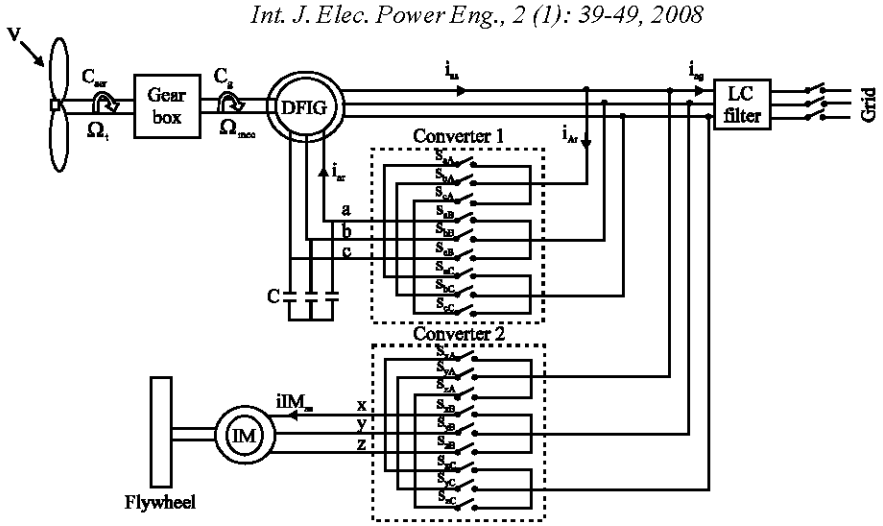

Fig. 1: Scheme of the studied device include the matrix converter topology

the flywheel energy storage system. The FESS considered for this application contains a flywheel and a classical squirrel-cage Induction Machine (IM). The IM operates in the flux-weakening region, the field-oriented control will be considered for the IM-based FESS (Hardan *et al*., 1998; Robyns *et al*., 2003). Finally, we present the study of the device using numerical simulation. The scheme of the studied device is given in the Fig. 1.

MODELING OF THE WIND GENERATOR

Modeling of the wind turbine and gearbox: The aerodynamic power, which is converted by a wind turbine, P_t is dependent on the power coefficient C_p. It is given by:

$$P_t = \frac{1}{2} C_p(\lambda) \rho \pi R^2 V^3 \quad (1)$$

Where ρ is the air density, R is the blade length and V the wind velocity.

The turbine torque is the ratio of the output power to the shaft speed

$$\Omega_t,\ C_{aer} = \frac{P_t}{\Omega_t}$$

The turbine is normally coupled to the generator shaft through a gearbox whose gear ratio G is chosen in order to set the generator shaft speed within a desired speed range. Neglecting the transmission losses, the torque and shaft speed of the wind turbine, referred to the generator side of the gearbox, are given by:

$$C_g = \frac{C_{aer}}{G} \text{ and } \Omega_t = \frac{\Omega_{mec}}{G} \quad (2)$$

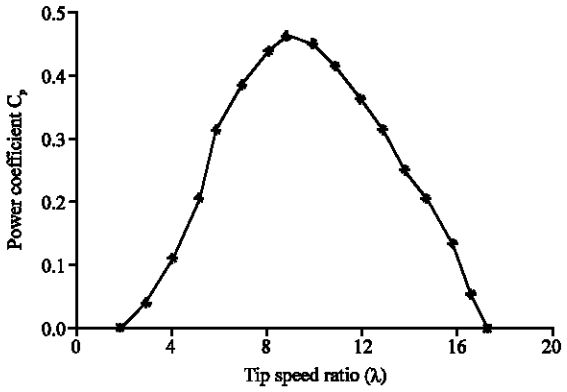

Fig. 2: Power coefficient for the wind turbine model (Aouzellag *et al*., 2006)

Where: C_g is the driving torque of the generator and Ω_{mec} is the generator shaft speed, respectively.

A wind turbine can only convert just a certain percentage of the captured wind power. This percentage is represented by $C_p(\lambda)$ which is function of the wind speed, the turbine speed and the pith angle of specific wind turbine blades (Aouzellag *et al*., 2006; Chang, 2002; Schuster, 1998).

Although this equation seems simple, C_p is dependent on the ratio λ between the turbine angular velocity Ω_t and the wind speed V.This ratio is called the tip speed ratio:

$$\lambda = \frac{\Omega_t R}{V} \quad (3)$$

A typical relationship between C_p and λ is shown in Fig. 2. It is clear from this figure that there is a value of λ for which C_p is maximum and that maximize the power for a given wind speed. The peak power for each wind speed

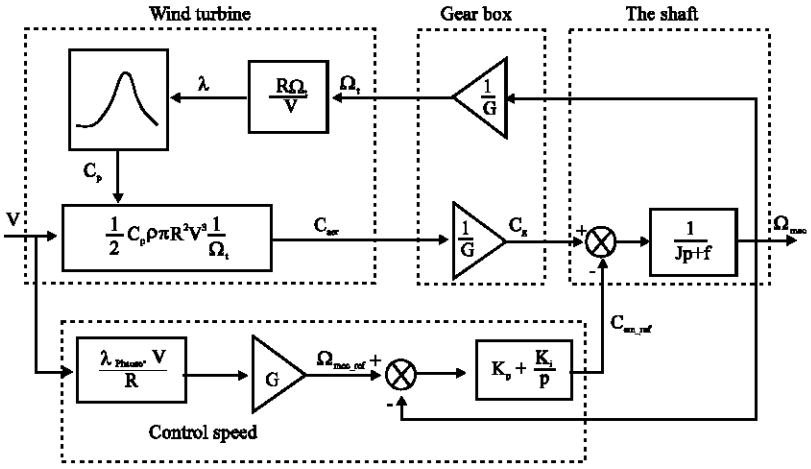

Fig. 3: Device control with control speed

occurs at the point where C_p is maximized. To maximize the generated power, it is therefore desirable for the generator to have a power characteristic that will follow the maximum C_{p_max} line.

The action of the speed corrector must achieve two tasks (Aimani, 2003):

- It must control the mechanical speed Ω_{mec} in order to yet a speed reference Ω_{mec_ref}.
- It must attenuate the action of the aerodynamic torque, which is an input disturbance.

The simplified representation in the form of diagram blocks is given on Fig. 3.

If the wind speed is measured and the mechanical characteristics of the wind turbine are known, it is possible to deduce in real-time the optimal mechanical power which can be generated using the Maximum Power Point Tracking (MPPT). The optimal mechanical power can be expressed as:

$$P_{mec\_opt} = -\frac{C_{p\_max}}{\lambda^2_{C_{p\_max}}}.\frac{\rho\pi R^5}{2}.\frac{\Omega^3_{mec}}{G^3} \quad (4)$$

Modeling of the DFIG: The classical electrical equations of the DFIG in the PARK frame are written as follows:

$$\begin{cases} V_{ds} = R_s i_{ds} + \dfrac{d}{dt}\phi_{ds} - \omega_s \phi_{qs} \\ V_{qs} = R_s i_{qs} + \dfrac{d}{dt}\phi_{qs} + \omega_s \phi_{ds} \\ V_{dr} = R_r i_{dr} + \dfrac{d}{dt}\phi_{dr} - (\omega_s - \omega)\phi_{qr} \\ V_{qr} = R_r i_{qr} + \dfrac{d}{dt}\phi_{qr} + (\omega_s - \omega)\phi_{dr} \end{cases} \quad (5)$$

Where, R and R_r are, respectively the stator and rotor phase resistances, $\omega = P.\Omega_{mec}$ is the electrical speed and P is the number of pair pole.

The stator and rotor flux can be expressed as:

$$\begin{cases} \phi_{ds} = L_s i_{ds} + L_m i_{dr} \\ \phi_{qs} = L_s i_{qs} + L_m i_{qr} \end{cases}, \begin{cases} \phi_{dr} = L_r i_{dr} + L_m i_{ds} \\ \phi_{qr} = L_s i_{qr} + L_m i_{qs} \end{cases} \quad (6)$$

Where, i_{ds}, $i_{\phi s}$, i_{dr} and i_{qr} are respectively the direct and quadrate stator and rotor currents.

The active and reactive powers at the stator, the rotor as well as those provide for grid are defined as:

$$\begin{cases} P_s = v_{ds}.i_{ds} + v_{qs}.i_{qs} \\ Q_s = v_{qs}.i_{ds} - v_{ds}.i_{qs} \end{cases} \quad (7)$$

$$\begin{cases} P_r = v_{dr}.i_{dr} + v_{qr}.i_{qr} \\ Q_r = v_{qr}.i_{dr} - v_{dr}.i_{qr} \end{cases} \quad (8)$$

$$\begin{cases} P_g = P_s + P_r \\ Q_g = Q_s + Q_r \end{cases} \quad (9)$$

The electromagnetic torque is expressed as:

$$T_{em} = P.(\phi_{ds}.i_{qs} - \phi_{qs}.i_{ds}) \quad (10)$$

MODELING OF THE MATRIX CONVERTER

Matrix converter consists of nine bidirectional switches which are considered ideal for the ease of this presentation (Aouzellag *et al.*, 2000; Han, 2004). Each

output phase is associated with three switches set connected to three input phases. This configuration of bidirectional switches enables the connection of any input phase a, b or c to any output phase A, B or C at any instant (Converter 1 Fig. 1). The switching function of a switch S_{ij} in Fig. 1 is defined (referred to converter1) as.

$$S_{ij}=\begin{cases}1 & S_{ij}\text{ is closed}\\ 0 & S_{ij}\text{ is open}\end{cases}\quad i\in\{a,b,c\},\ j\in\{A,B,C\},\tag{11}$$

The switching angles formulation: The switching angles, of the nine bidirectional switches S_{ij} witch will be calculated, must comply with the following rules:

- At any time 't', only one switch S_{ij}(j=1,2,3) will be in 'ON' state. This assures that no short circuit will occur at the input terminals.
- At any time 't', at least two of the switches S_{ij} (I = 1,2,3) will be in 'ON' state. This condition guarantees a closed-loop path for the load current (usually this is an inductive current).

During the k^{th} switching cycle T_s ($T_s=1/f_s$) Fig. 4, the first phase output voltage is given by:

$$v_a=\begin{cases}v_A & 0\le t-(k-1)T_s<m_{aA}^k T_s\\ v_B & m_{aA}^k T_s\le t-(k-1)T_s<\left(m_{aA}^k+m_{aB}^k\right)T_s\\ v_C & \left(m_{aA}^k+m_{aB}^k\right)T_s\le t-(k-1)T_s<T_s\end{cases}\tag{12}$$

Where 'm's are defined by:

$$m_{ij}^k=\frac{t_{ij}^k}{T_s}\tag{13}$$

Where t_{ij}^k: Time interval when S_{ij} is in 'ON' state, during the k^{th} cycle and k is being the switching cycle sequence number. The 'm's have the physical meaning of duty cycle.
Also,

$$m_{iA}^k+m_{iB}^k+m_{iC}^k=1\quad\text{and } 0<m_{ij}^k<1$$

Which means that during every cycle T_s all switches will turn on and off once.

Algorithm of Venturini: The algorithm of Venturini (1980) and Alesina and Venturini (1988), allows a control of the S_{ij} switches so that the low frequency parts of the synthesized output voltages (v_a, v_b and v_c) and the input currents (i_{Ar}, i_{Br} and i_{Cr}) are purely sinusoidal with the prescribed values of the output frequency, the input

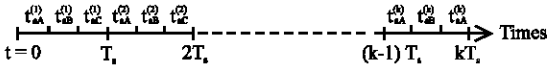

Fig. 4: Segmentation of the axis time for the consecutive orders of intervals closing of the switches

frequency, the displacement factor and the input amplitude. The average values of the output voltages during the k^{th} sequence re thus given by:

$$\begin{cases}v_a=\frac{t_{aA}^k}{T_s}v_A+\frac{t_{aB}^k}{T_s}v_B+\frac{t_{aC}^k}{T_s}v_C\\ v_b=\frac{t_{bA}^k}{T_s}v_A+\frac{t_{bB}^k}{T_s}v_B+\frac{t_{bC}^k}{T_s}v_C\\ v_c=\frac{t_{cA}^k}{T_s}v_A+\frac{t_{cB}^k}{T_s}v_B+\frac{t_{cC}^k}{T_s}v_C\end{cases}\tag{14}$$

If times of conduction are modulated in the shape of sinusoidal with the pulsation W_m while T_s remains constant, such as w_o w_i + w_m, these times are defined as fellows:

- For the 1st phase, we have:

$$\begin{cases}t_{aA}=\frac{T_s}{3}\left(1+2q\cos(w_m t+\theta)\right)\\ t_{aB}=\frac{T_s}{3}\left(1+2q\cos(w_m t+\theta-\frac{2\pi}{3})\right)\\ t_{aC}=\frac{T_s}{3}\left(1+2q\cos(w_m t+\theta-\frac{4\pi}{3})\right)\end{cases}\tag{15}$$

- For the 2nd phase:

$$\begin{cases}t_{bA}=\frac{T_s}{3}\left(1+2q\cos(w_m t+\theta-\frac{4\pi}{3})\right)\\ t_{bB}=\frac{T_s}{3}\left(1+2q\cos(w_m t+\theta)\right)\\ t_{bC}=\frac{T_s}{3}\left(1+2q\cos(w_m t+\theta-\frac{2\pi}{3})\right)\end{cases}\tag{16}$$

- For the 3rd phase:

$$\begin{cases}t_{cA}=\frac{T_s}{3}\left(1+2q\cos(w_m t+\theta-\frac{2\pi}{3})\right)\\ t_{cB}=\frac{T_s}{3}\left(1+2q\cos(w_m t+\theta-\frac{4\pi}{3})\right)\\ t_{cC}=\frac{T_s}{3}\left(1+2q\cos(w_m t+\theta)\right)\end{cases}\tag{17}$$

Where θ is the initial phase angle.
The output voltage is given by:

$$\begin{bmatrix} v_a \\ v_b \\ v_c \end{bmatrix} = \begin{bmatrix} 1+2q\cos\alpha & 1+2q\cos\left(\alpha-\frac{2\pi}{3}\right) & 1+2q\cos\left(\alpha-\frac{4\pi}{3}\right) \\ 1+2q\cos\left(\alpha-\frac{4\pi}{3}\right) & 1+2q\cos\alpha & 1+2q\cos\left(\alpha-\frac{2\pi}{3}\right) \\ 1+2q\cos\left(\alpha-\frac{2\pi}{3}\right) & 1+2q\cos\left(\alpha-\frac{4\pi}{3}\right) & 1+2q\cos\alpha \end{bmatrix} \cdot \begin{bmatrix} V_A \\ V_B \\ V_C \end{bmatrix} \quad (18)$$

$$\text{Where}: \begin{cases} a = w_m t + \theta \\ w_m = w_o - w_i \end{cases}$$

The running matrix converter with Venturini algorithm generates at the output a three-phases sinusoidal voltages system having in that order pulsation w_m, a phase angle θ and amplitude q.Vs (0<q<0.866 with modulation of the neutral) (Venturini, 1980).

SYSTEM CONTROL

The system of the studied device (Fig. 5) included two control blocs (DFIG control and FFSS control). The first one is deduced to control the active and reactive power exchanged between the grid and DFIG. The last one is deduced to control the energy storage in the flywheel. Those blocs can be controlled independently.

Active and reactive DFIG power control: When the DFIG is connected to an existing grid, this connection must be done in three steps. The first step is the regulation of the stator voltages with the grid voltages as reference. The second step is the stator connection to this grid. As the voltages of the two devices are synchronized, this connection can be done without problem. Once this connection is achieved, the third step is the transit power regulation between the DFIG and the grid (Fig. 5).

We choose a d-q reference-frame synchronized with the stator flux (Muljadi, 1998). By setting null the quadratic compound of the stator:

$$\Phi_{ds} = \Phi_s \text{ and } \Phi_{qs} = 0 \quad (19)$$

Then the torque is simplified into:

$$T_{em} = -P\frac{L_m}{L_s} I_{qr} \Phi_{ds} \quad (20)$$

The electromagnetic torque and then the active power will only depend on the q-axis rotor current. By neglecting the stator resistance R_s, we can write:

$$V_{ds} = 0 \text{ and } V_{qs} = V_s \quad (21)$$

In order to calculate angles for the Park transformation for stator and rotor variables, the stator pulsation and the mechanical speed must be sensed.

By choosing this reference frame, stator voltages and fluxes can be rewritten as follows:

$$\begin{cases} V_{ds} = 0 & ; \; V_{qs} = V_s = \omega_s \Phi_{ds} \\ \Phi_{ds} = \Phi_s = L_s I_{ds} + L_m I_{dr} & ; \; \Phi_{dr} = L_r I_{dr} + L_m I_{ds} \\ \Phi_{qs} = 0 = L_s I_{qs} + L_m I_{qr} & ; \; \Phi_{qr} = L_r I_{qr} + L_m I_{qs} \end{cases} \quad (22)$$

The stator active and reactive power, the rotor voltages can be written according to the rotor currents as:

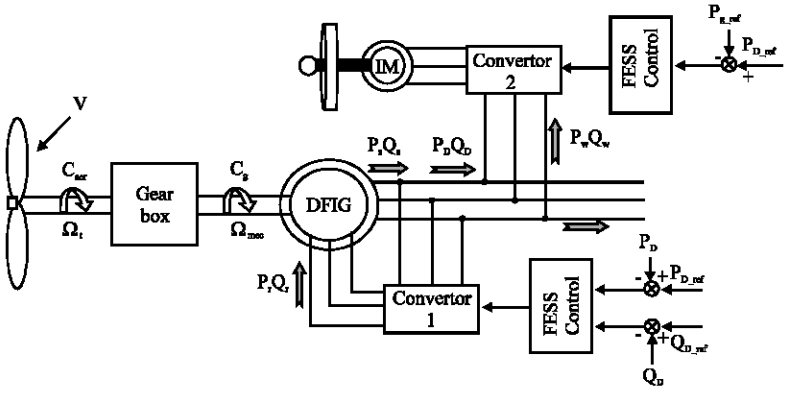

Fig. 5: Scheme of the system

$$\begin{cases} P_s = -V_s \dfrac{L_m}{L_s} I_{qr} \\ Q_s = \dfrac{V_s \phi_s}{L_s} - \dfrac{V_s L_m}{L_s} I_{dr} \end{cases} \quad (23)$$

$$\begin{cases} V_{dr} = R_r I_{dr} + \left(L_r - \dfrac{L_m^2}{L_s} \right) \dfrac{dI_{dr}}{dt} - s.\omega_s \left(L_r - \dfrac{L_m^2}{L_s} \right) I_{qr} \\ V_{qr} = R_r I_{qr} + \left(L_r - \dfrac{L_m^2}{L_s} \right) \dfrac{dI_{qr}}{dt} + s.\omega_s \left(L_r - \dfrac{L_m^2}{L_s} \right) I_{dr} + s.\omega_s \dfrac{L_m V_s}{\omega_s L_s} \end{cases} \quad (24)$$

With $s = \dfrac{\omega_s - \omega}{\omega_s}$

For slip values relatively weak, the expression (9) can be simplified as follows:

$$\begin{cases} P_D = (s-1).V_s.\dfrac{L_m}{L_s}.I_{qr} \\ Q_D = \dfrac{V_s^2}{\omega_s.L_s} + (s-1).V_s.\dfrac{L_m}{L_s}.I_{dr} \end{cases} \quad (25)$$

In steady state, the second derivative terms of both Eq. (24) are nulls. The third terms are cross-coupling terms and can be neglected because of their small influence. Knowing relation (25), it is possible to design the regulators. The global block-diagram of the controlled system is depicted on Fig. 6.

The blocks R_P and R_Q represent active and reactive power regulators. The aim of these regulators is to obtain high dynamic performances in terms of reference tracking, sensitivity to perturbations and robustness (Muljadi, 1998).

Control of a FESS associated to a VSWG

Control strategy for the FESS: The wind generators are considered as negative charges for the power grid because they do not consume the electric energy but generate it without participating to the ancillary services. It is well known that the wind speed is very fluctuant and, by this reason, the wind deliver a variable electrical power. Tot overcome this drawback, the acting on the electrical system is enough, e.g. associating an energy storage system with the wind generator in order to regulate the electric power delivered into the grid (Pena *et al*., 2001).

If P_g is the power expected from the coupling VSWG-FESS assembly and P_{men_opt} the optimal aerodynamic power generated by the wind, the reference value P_{D_ref} of the DFIG active power is determined by

$$P_{D\_ref} = \eta.P_{mec\_opt} \quad (26)$$

The reference value P_{w_ref} of the active power exchanged between the FESS and the grid is determined by

$$P_{w\_ref} = \eta.P_{mec\_opt} - P_{g\_ref} \quad (27)$$

Where: ηrepresent the efficiency of the IM, it is estimated to 95% and P_{g_ref} is the reference grid active power, fixed to the value -1.5MW.

Induction machine modelling: The IM, modelled in the Park reference frame, is described by (28)-(32):

$$\begin{aligned} v_{sd_{IM}} &= R_{s_{IM}} i_{sd_{IM}} + \sigma_{IM}.L_{s_{IM}} \frac{di_{sd_{IM}}}{dt} \\ &+ \frac{M_{IM}}{L_{r_{IM}}} \frac{d\phi_r}{dt} - \omega_s.\sigma_{IM}.L_{s_{IM}} i_{sq_{IM}} \end{aligned} \quad (28)$$

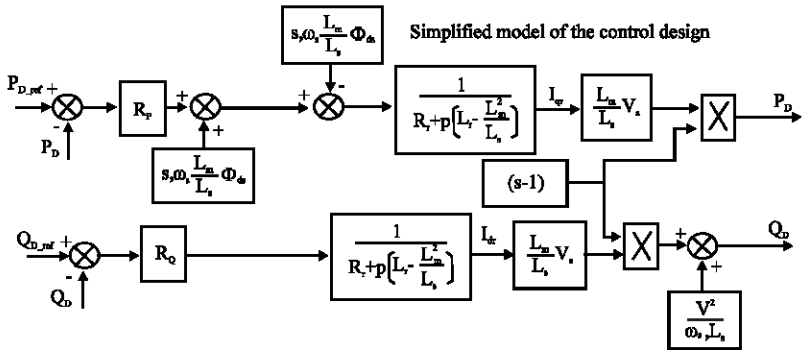

Fig. 6: Block diagram of DFIG power control

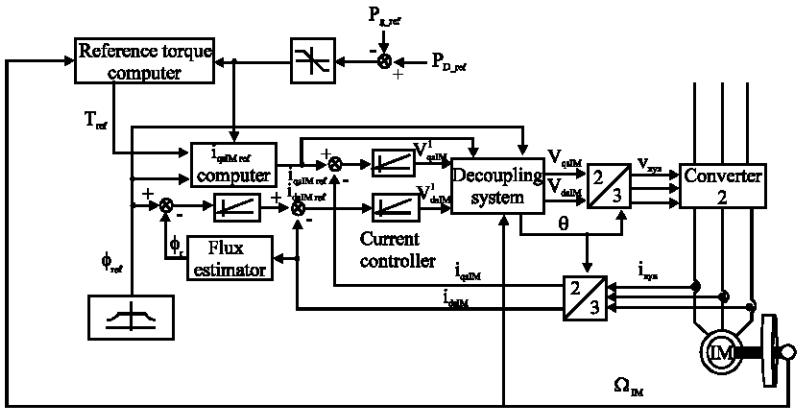

Fig. 7: FESS induction machine control scheme

$$v_{sq_{IM}} = R_{s_{IM}}.i_{sq_{IM}} + \sigma_{IM}.L_{s_{IM}}\frac{di_{sq_{IM}}}{dt} + \frac{M_{IM}}{L_{r_{IM}}}\frac{d\phi_r}{dt} + \omega_s.\sigma_{IM}.L_{s_{IM}}.i_{sd_{IM}} \quad (29)$$

$$M_{IM}.i_{sd_{IM}} = \phi_r + \frac{L_{rIM}}{R_{r_{IM}}}\frac{d\phi_r}{dt} \quad (30)$$

$$\omega_s = p_{IM}.\Omega_{IM} + \frac{M_{IM}.R_{r_{IM}}}{L_{r_{IM}}}\frac{i_{sq_{IM}}}{\phi_r} = p_{IM}.\Omega_{IM} + \omega_{sr} \quad (31)$$

$$T_{emIM} = p_{IM}\frac{M_{IM}}{L_{r_{IM}}}\phi_r.i_{sqIM} \quad (32)$$

All the parameters of the preceding equations are defined in the appendix.

Flux-weakening operation of the FESS induction machine: The IM being under rotor flux-oriented control, the corresponding power equation is determined as

$$P_{IM} = T_{emIM}.\Omega_{IM} = p_{IM}\frac{M_{IM}}{L_{r_{IM}}}\phi_{rd}.i_{sq_{IM}}.\Omega_{IM} \quad (33)$$

Where P_{IM} defines the electric power, T_{emIM} the electromagnetic torque, Ω_{IM}, the mechanical speed, p_2, the pole-pair number, M_{IM}, the mutual inductance, L_{rIM}, the rotor inductance, ϕ_{rd}, the d-axis rotor-flux component, i_{sqIM}, the q-axis component of the stator current.

From Eq. 33, the rotor-flux reference value can be computed as

$$\phi_{rdref} = \frac{P_{IM}.L_{r_{IM}}}{p_{IM}.M_{IM}.i_{sq_{IM}max}}.\frac{1}{\Omega_{IMmes}} \quad (34)$$

Control of the FESS induction machine: The torque control is used for the FESS induction machine. The reference power of the FESS, P_{wref}, must be saturated to the rated value of the IM power in order to avoid the IM overheating. The torque reference is given by:

$$T_r = \frac{P_w}{\Omega_{IM}} + B.\Omega + T_s \quad (35)$$

Where P_w is computed by Eq.(27), T_s is the static torque and B, the viscous friction coefficient. From Eq. (33-35), the reference current results as

$$i_{sq_{IM}ref} = \frac{T_r.L_{r_{IM}}}{p_{IM}.M_{IM}.\phi_r} \quad (36)$$

The control scheme of the induction machine is presented in Fig. 7.

RESULTS AND DISCUSSION

We present the simulation of the DFIG connected directly to the grid through the stator and controlled through its rotor circuit an AC/AC direct converter. To control the power exchanged between the wind generator and the grid, one uses the vector control with direct stator flux. The reference value P_{w_ref} of the active power exchanged between the FESS and the grid is determined by the Eq. (27). The torque control is used for the FESS induction machine.

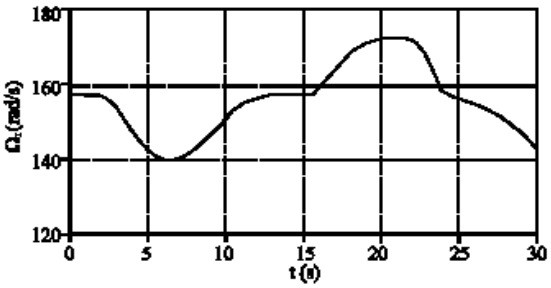

Fig. 8: Random of the DFIG rotor speed

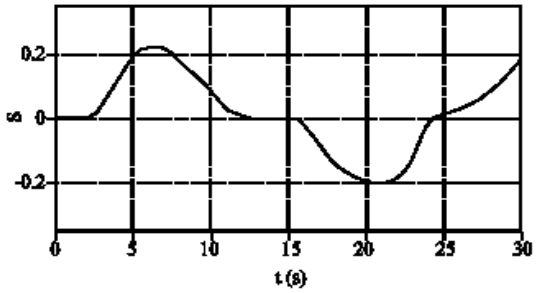

Fig. 9: DFIG slip s

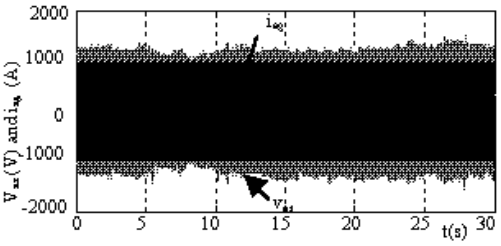

Fig. 10a: Grid voltage and current

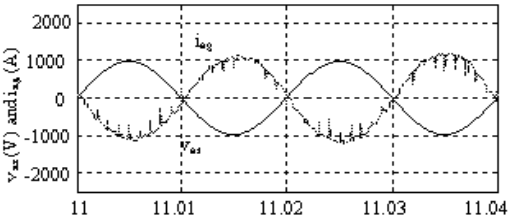

Fig.10b: Zoom of the grid voltage and current

The results of simulations are obtained with reactive power Q_{g_ref} and active power P_{g_ref} Figure 8 and 9 show respectively the angular speed random and the slip of the DFIG. Figure 10a shows the grid voltage and current waveforms. Note that the sinusoidal current, in phase opposition compared to the voltage (Fig. 10b), the machine supplies grid with active power. The sizes (grid current and voltage) are independent of the variation of the wind and depend only on the active and reactive

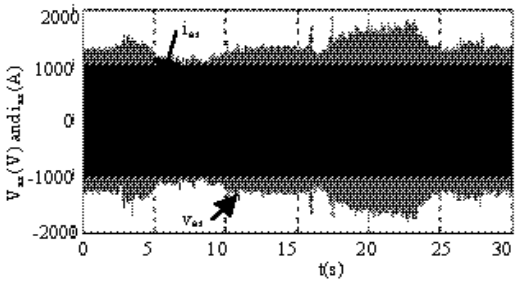

Fig. 11a: Stator voltage and current

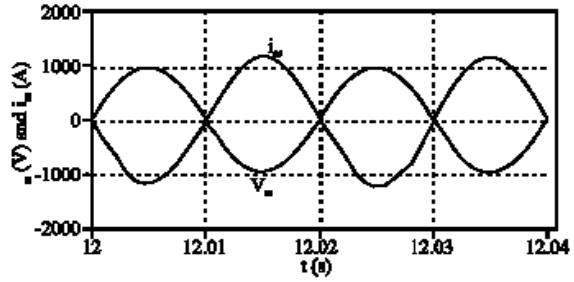

Fig. 11b: Zoom of stator voltage and current

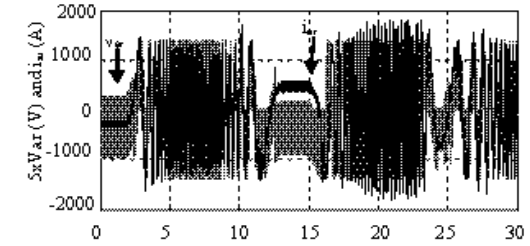

Fig. 12a: Rotor voltage and current

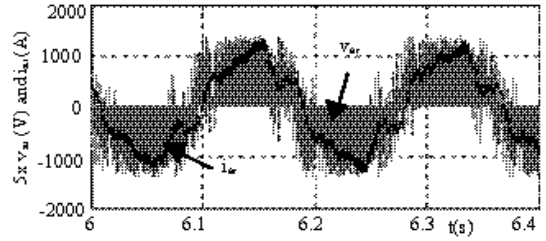

Fig. 12.b: Zoom rotor voltage and current for s > 0

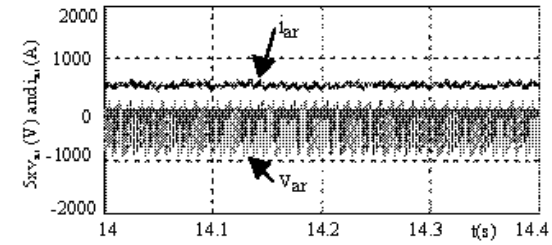

Fig. 12c: Zoom rotor voltage and current for s = 0

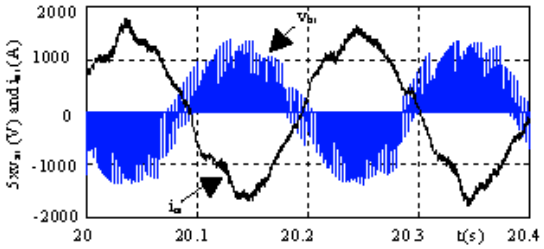

Fig. 12d: Zoom rotor voltage and current for s < 0

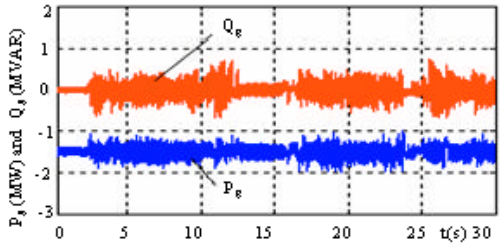

Fig. 13: Grid active and reactive powers

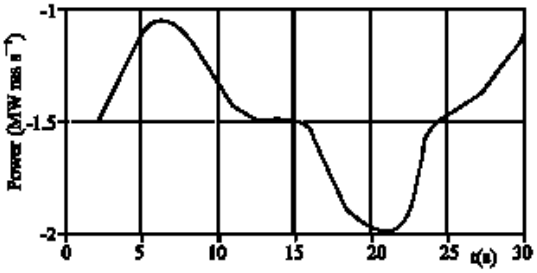

Fig. 14: Wind generator power $_{Pmec}$

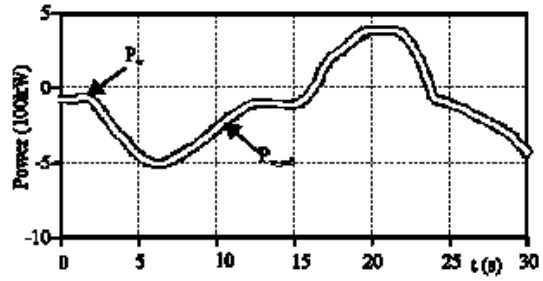

Fig. 15: Reference power $_{Pw\_ref}$ and delivered IM power P_w

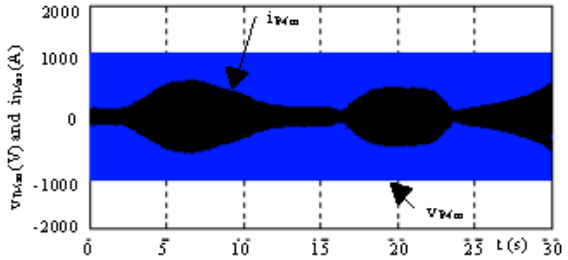

Fig. 16a: Stator voltage and current of IM

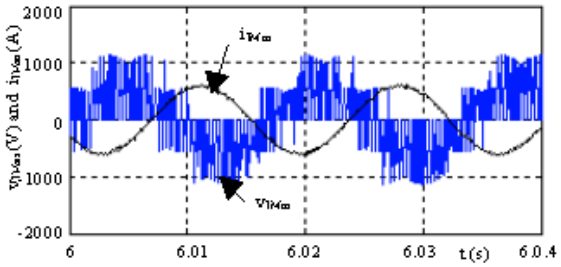

Fig. 16b: Zoom stator voltage and current of IM

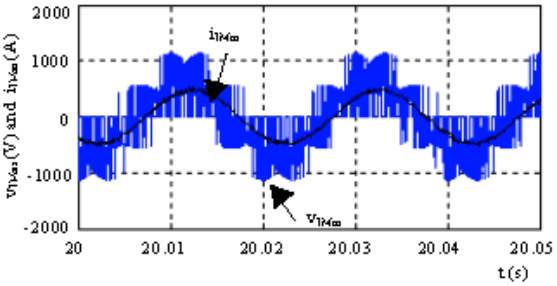

Fig. 16c: Zoom stator voltage and current of IM

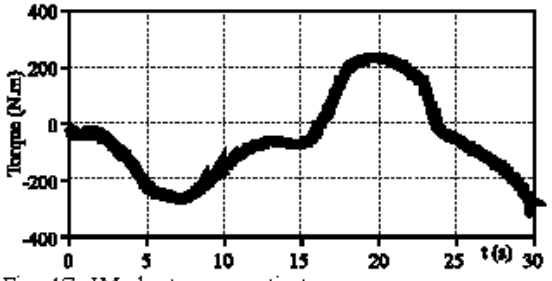

Fig. 17: IM electromagnetic torque

reference powers. The stator voltage and current waveforms and these zoom are show, respectively in Fig. 11a and b. Figure 12a shows the rotor voltage and current waveforms. The frequency of these voltage and current, vary according to the slip s (Fig. 12b-d). For s = 0, the rotor voltage and current are continuous. Figure 13 gives grid active and reactive powers. The grid powers follow their references perfectly. Figure 14 shows the variation of the mechanical power according to the generator speed. Figure 14 show the FESS powers P_w and those reference power P_{w_ref}. The Stator voltage and current waveforms and these zoom of the IM are show respectively in Fig 16a, b and c. Figure 17 shows the IM electromagnetic

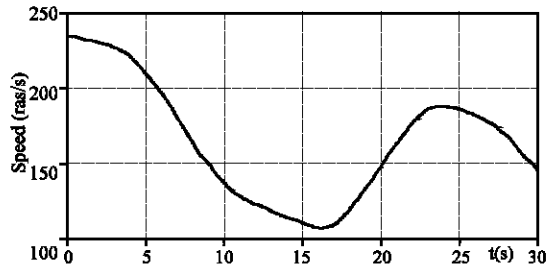

Fig. 18: Flywheel speed

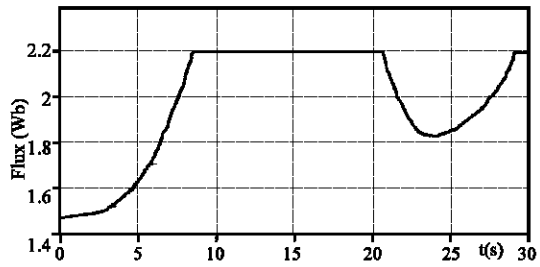

Fig. 19: Magnitude of IM stator flux

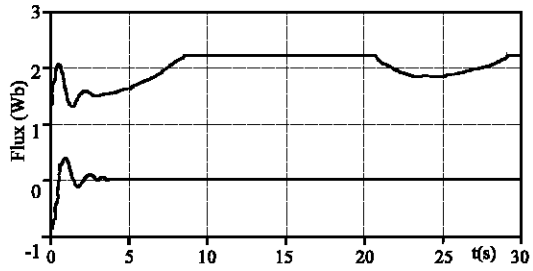

Fig. 20: Direct and quadratic magnitude of IM rotor flux

torque witch is very fluctuant, like the wind generated power and entails the freewheeling speed (Fig. 18). The IM operates in the flux weakening region and the magnitude of its stator flux changes as a function of the speed (Fig. 19). Figure 20 shows the decoupling between direct and quadratic rotor flux of the IM.

CONCLUSION

A Variable Speed Wind Generator (VSWG) associated to a Flywheel Energy Storage System (FESS) has been described in this study. The first part is devoted to the analysis, modelling and simulation of a variable speed wind turbine using a doubly fed induction generator in conjunction with the matrix converter. Stable operation of the DFIG was achieved by means of stator-flux oriented control technique. The operational principal of the proposed wind-power generator model and the validity of the control system were illustrated by the steady-state and transient responses of the power control associated to the DFIG. In the second part the FESS with IM is developed.

Simulation results have been carried out, validating on the one hand, each part of the system, on the other hand, the FESS concept associated to a VSWG.

The DFIG operates in two quadrants. For $s > 0$, DFIG operates in sub-synchronous. For $s < 0$, DFIG operate in super-synchronous model. For $s = 0$, DFIG operates as synchronized asynchronous generator and the rotor voltage and currents are continuous. The machine supplies grid with an active power in all operating modes.

The overall dynamic performance of the system shows that the MC is technically a viable to the conventional AC-DC-AC converter system as the interface unit of the wind generator system.

Appendix 1:

The Turbine

Ω_{mec}	=	Mechanical speed of the DFIG.
Ω_{mec_ref}	=	Mechanical speed reference.
Ω_t	=	Turbine speed.
P_{mec_opt}	=	Mechanical optimal.
C_{ear}	=	Aerodynamic torque.
C_g	=	Generator torque.
s	=	Generator slip.
C_p	=	Power coefficient.
λ	=	Tip speed ratio.
ρ	=	Air density.
R	=	Turbine radius.
V	=	Wind velocity.
G	=	Gear ratio.

The DFIG

V_{ds}, V_{qs}, V_{dr}, V_{qr}	=	Two-phase stator and rotor voltages.
ϕ_{ds}, ϕ_{qs}, ϕ_{dr}, ϕ_{qr}	=	Two-phase stator and rotor fluxes.
I_{ds}, I_{qs}, I_{dr}, I_{qr}	=	Two-phase stator and rotor currents.
R_s , R_r	=	Per phase stator and rotor resistances.
L_s, L_r	=	Total cyclic stator and rotor inductances.
L_m	=	Magnetizing inductance.
P	=	Number of pole pairs.
J	=	Inertia.
f	=	Viscous friction.
p	=	Laplace operator.
P_s, Q_s	=	Active and reactive stator power.
P_r, Q_r	=	Active and reactive rotor power.
P_D, Q_D	=	Active and reactive DFIG power.
P_g, Q_g	=	Active and reactive grid power.

The IM and flywheel

p_{IM}	=	Pole pairs.
R_{sIM}	=	Stator resistance.
R_{rIM}	=	Rotor resistance.

M_{IM} = Mutual inductance.
L_{sIM} = Stator inductance.
L_{rIM} = Rotor inductance.
σ_{IM} = Dispersion ratio.
J_F = FESS inertia (Flywheel+IM).
$P_{w\text{-}ref}$ = Reference of IM active power
P_w = Active power exchanged between the FESS and the grid.
Q_w = Reactive power exchanged between the FESS and the grid.
B = Viscous friction coefficient.
T_{st} = Static torque.
v_a, v_b, v_c = Output phase voltages.
v_A, v_B, v_C = Input phase voltages.
i_a, i_b, i_c = Output phase currents.
i_A, i_B, i_C = Input phase currents.
S_{ij} = Switch function.
T_s = Switching interval.
θ_i = Angle of the reference input current vector.
θ_o = Angle of the reference output voltage vector.

REFERENCES

Alesina, A. and M. Venturini, 1988. Intrinsic amplitude limits and optimum design of 9 switches direct PWM ac-ac converter. Proc. PSEC. Conf., pp: 1284-1290.

Ansel, A. and B. Robyns, Modelling ans simulation of an autonomous variable speed micro hydropower station, Mathematics and Computers in Simulation Journal No.71.

Aouzellag, D., K. Ghedamsi and E.M. Berkouk, 2006. Modeling of Doubly Fed Induction Generator with Variable Speed Wind turbine for Network Power Flow Control, WSEAS J. Issue 12: 1995-2000, ISSN 1790-5060.

Aouzellag, D., K.Ghedamsi and E.M. Berkouk, 2006. Modelling of Doubly Fed Induction Generator with Variable Speed Wind for Network Power Flow Control. JTEA, Tunis.

Aouzellag, D., K.Ghedamsi and E.M. Berkouk, 2006. Power Control of a Variable Speed Wind Turbine Driving an DFIG. ICREPQ'06, Spain.

Barton, J.P. and D.G. Infield, 2004. Energy Storage and its Use With Intermittent Renewable Energy. IEEE. Trans. Energy Conversion, 19: 441-448.

Cadenas, R., R. Pena, G. Asher, J. Clare and R. Blasco-Giménez, 2001. Control strategies for enhanced power smoothing in wind energy systems using a flywheel driven by a vector-controlled induction machine. IEEE. Trans. Indus. Elec., 48: 625-635.

Chang, L., 2002. Systemes de conversion de l'énergie éolienne. IEEE. Can. Rev. Summer, pp: 1-5.

Cimuca, G., M.M. Radulescu, C. Saudemont and B. Robyns, 2004. Performance Analysis of an Induction Machine-Based Flywheel Energy Storage System Associated to a Variable-Speed Wind Generator, Proceedings of the 9th International Conference on Optimization of Electrical and Electronic Equipments. OPTIM, Brasov, Romania, II: 319-326.

El Aimani, S., 2003. Modelling and simulation of doubly fed induction generator for variable speed wind turbines integrated in a distribution network, 10th European Conference on power Electronics and Application, Toulouse, France.

Ghedamsi, K., D. Aouzellag and E.M. Berkouk, 2006. Application of Matrix Converter for Variable Speed Wind Turbine Driving an Doubly Fed Induction Generator, SPEEDAM, Italy.

Han Ju Cha, 2004. Analysis and design of matrix converter for adjustable speed drives and distributed power sources, PhD thesis, Texas A and M University.

Hardan, F., J.A.M. Bleijs, R. Jones, P. Bromley, 1998. Bi-directional power control for flywheel energy storage system with vector-controlled induction machine drive. IEEE. Conf. Pub., pp: 456-477.

Hebner, R. and J. Beno, 2002. A.Walls, Flywheel batteries come around again. IEEE. Spectrum, pp: 44-51.

Leclercq, L.B. and Robyns, J.M. Grave, 2003. Control Based on fuzzy logic of a flywheel energy storage system associated with wind and diesel generators, Mathematics and Computers in Simulation, 63: 271-280.

Lawrence, R.G., K.L. Craven, G.D. Nickols and U.P.S. Flywheel, 2003. IEEE. Indus. Application Mag., pp: 44-50.

Muljadi, E.K. Pierce and P. Migliore, 1998. Control strategy for variable-speed, stall-regulated wind turbines, in the Proceeding of American Controls Conference, Philadelphia, PA., pp: 1-8.

Schuster, A., 1998. Commande, réglage et optimisation d'un convertisseur matriciel pour entraînement par moteur asynchrone, Doctorat Thesis L'EPLF, LEI Lausanne.

Seyoum, D. and C. Grantham, 2003. Terminal voltage control of a wind turbine driven isolated induction generator using stator oriented field control. IEEE. Trans. Indus. Applications, pp: 846-852.

Tounzi, A., 1998. Utilisation de l'énergie éolienne dans la production de l'électricité, Journées du club EEA, Paris (France), pp: 1-14.

Venturini, M., 1980. The generalized transformer: a new bidirectional sinusoidal waveform, frequency converter with continuously adjustable input power factor. Proc. PESC., pp: 242-252.